JOURNAL OF MATERIALS SCIENCE **34** (1999) 1991–1997

Grain boundary bonding state and fracture energy in small amount of oxide-doped fine-grained Al_2O_3

Y. TAKIGAWA*, Y. IKUHARA, T. SAKUMA
Department of Materials Science, Faculty of Engineering, The University of Tokyo, 7-3-1 Hongo, Bunkyo-ku, Tokyo 113-8656, Japan
E-mail: ikuhara@ceramic.mm.t.u-tokyo.ac.jp

Grain boundary structure and chemical bonding state were characterized in high-purity Al_2O_3, 0.1 wt % MgO, 0.1 wt % Y_2O_3 or 0.1 wt % ZrO_2-doped Al_2O_3. High resolution electron microscopy (HREM) and energy dispersive X-ray spectroscopy (EDS) revealed that all samples examined have single phase structure, and that doped cations segregate along grain boundaries. Electron energy loss spectroscopy (EELS) spectra taken from grain boundaries in doped Al_2O_3 shows slight chemical shift in comparison with those from grain interior. This result suggests that the chemical bonding state in grain boundaries changes by the segregated ions. The change in chemical bonding state seems to affect the grain boundary fracture energy of Al_2O_3.

1. Introduction

High-temperature plastic flow in polycrystalline Al_2O_3 is sensitively affected by a small amount of dopant. The addition of 0.1 wt % MgO markedly improves the high-temperature tensile ductility in high-purity Al_2O_3 [1]. High-temperature creep rate of fine-grained Al_2O_3 is highly suppressed by the doping of 0.1 wt % ZrO_2 [2, 3]. The dopant effect in Al_2O_3 has been previously explained from the formation of second phase [2], but more recent data clarifies that the effect is mainly caused by grain boundary segregation [3, 4]. However, it is still hard to explain the macroscopic mechanical properties in terms of local grain boundary segregation. We need much information such as atomic structure, chemical composition, chemical bonding states of grain boundaries etc. for understanding the segregation effect on mechanical properties such as the high-temperature plastic flow.

High-resolution electron microscopy (HREM) is one of the most useful techniques to analyze the atomic structure of grain boundaries in fine-grained ceramics. In addition to the structural investigation by HREM, modern analytical techniques such as energy dispersive X-ray spectroscopy (EDS), electron energy loss spectroscopy (EELS) are useful to evaluate microscopically the chemical composition and the chemical bonding state at and on the grain boundaries in the ceramics.

In this study, the segregation effect is investigated in a small amount of oxide-doped Al_2O_3 by grain boundary analyses mentioned above, and the obtained results are compared with the grain boundary fracture energy.

2. Experimental

The composition of the samples examined in this study is high-purity Al_2O_3, Al_2O_3-0.1 wt % MgO, Al_2O_3-0.1 wt % Y_2O_3 and Al_2O_3-0.1 wt % ZrO_2, respectively. High-purity Al_2O_3 powders were supplied by Taimei Chemical Co. Ltd. (TM-DAR), MgO powders by Ube Chemical Co. Ltd., Y_2O_3 powders by Dowa Mining Co. Ltd. and ZrO_2 powders by Tosho Co. Ltd. Al_2O_3 powders were mixed with the dopant powders in a ball mill for 24 h and then dried and shifted through a 60 mesh sieve for granulation. The green compacts were prepared by pressing these powders under a pressure of 33 MPa, and further by cold-isostatically pressing under 100 MPa. Sintering was conducted at 1300 °C for high-purity Al_2O_3 and MgO-doped Al_2O_3, and at 1400 °C for Y_2O_3-doped and ZrO_2-doped Al_2O_3 for 2 h in air.

Single edge notched beam (SENB) method was applied for evaluating the grain boundary fracture energy. The specimens for SENB tests were cut to a size of $3 \times 4 \times 23$ mm^3 and their surface was mechanically polished. Then, straight notch was introduced at the center of the tensile surface by means of a diamond cutter with a slot width of 0.1 mm. The relative notch length (a) against width (W), a/W was fixed in the range 0.5 ± 0.05. The fracture tests were performed by a three-point bend geometry with a span of 16 mm at a crosshead speed of 0.02 mm/min at 400 °C in air in order to have complete grain boundary fracture. The K_{Ic} values were obtained from the average of five samples in each material.

* *Present address*: Research and Development Laboratory, Japan Fine Ceramics Center, 2-4-1 Mutsuno, Atsuta-ku, Nagoya, 468-8587 Japan.

The samples for TEM observations were cut into plates with a size of about $2 \times 2 \times 0.5$ mm^3, polished to a thickness of about 0.1 mm, and then attached by epoxy to stainless steel rings for reinforcement. Subsequently, they were polished to a thickness of about 50 μm and finally thinned by ion beam sputtering at a voltage of 5 kV. HREM were made using a Topcon EM002BF (200 kV) and JEOL JEM2010F (200 kV) field-emission type transmission electron microscopes with a point-to-point resolution better than 0.18 nm. Chemical analysis for grain boundaries was carried out by EDS using Noran Voyager system with the probe size less than 1 nm in the electron microscopes. EELS was applied in the JEM2010F (200 kV) TEM equipped with Gatan PEELS spectrometer (model 666) in order to evaluate the chemical bonding state at grain boundaries.

3. Results and discussion

3.1. Microstructure and chemical composition at grain boundaries

Fig. 1 shows the TEM micrographs of (a) high-purity Al_2O_3, (b) MgO-doped Al_2O_3, (c) Y_2O_3-doped Al_2O_3 and (d) ZrO_2-doped Al_2O_3 in an as-sintered state. The sintered bodies with relative density of more than 99% were obtained in all materials. The grains are fine and equiaxed in all materials. No second phase particles are observed in any oxide doped-Al_2O_3, although the solubility of Y_2O_3 or ZrO_2 into Al_2O_3 is negligibly small [5, 6], and that of MgO is much limited at the respective sintering temperature [7].

Fig. 2 is the high-resolution electron micrographs of grain boundaries in the three doped Al_2O_3. As seen in the micrographs, neither second phases nor an amorphous phase are observed along the grain boundaries in all materials. Second phase particles were not observed even at grain boundary multiple junctions.

Fig. 3 shows the typical EDS profiles obtained from grain interiors and grain boundaries in the three doped Al_2O_3. The spectra of the grain interiors were taken at about 10 nm apart from grain boundaries, and the electron probe size used for the analyses was approximately 1 nm. The presence of Mg^{2+}, Y^{3+} and Zr^{4+} ions is detected at the grain boundaries, but not at the grain interiors. This result indicates that the doped cations segregate in grain boundaries.

3.2. Grain boundary fracture energy

The segregation of doped cations in grain boundaries will affect the grain boundary fracture energy,which is related to the grain boundary energy. Several methods have been proposed to estimate the fracture energy in ceramics [8–11]. Among them, the method using fracture toughness K_{Ic} is very convenient and accurate enough to obtain the fracture energy of the present materials. SENB technique was utilized for estimating the

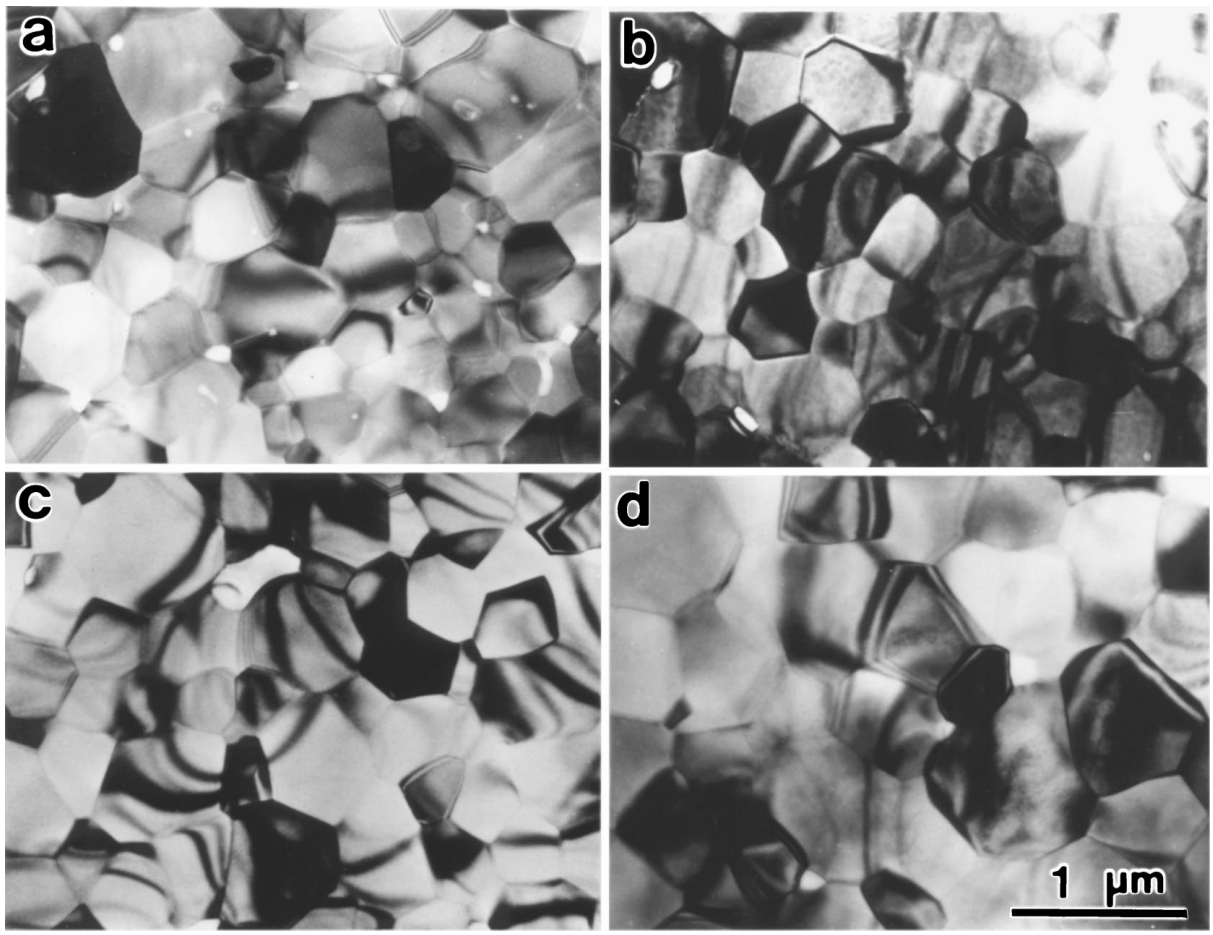

Figure 1 TEM micrographs of (a) high-purity Al_2O_3, (b) MgO-doped Al_2O_3, (c) Y_2O_3-doped Al_2O_3 and (d) ZrO_2-doped Al_2O_3 in an as-sintered state.

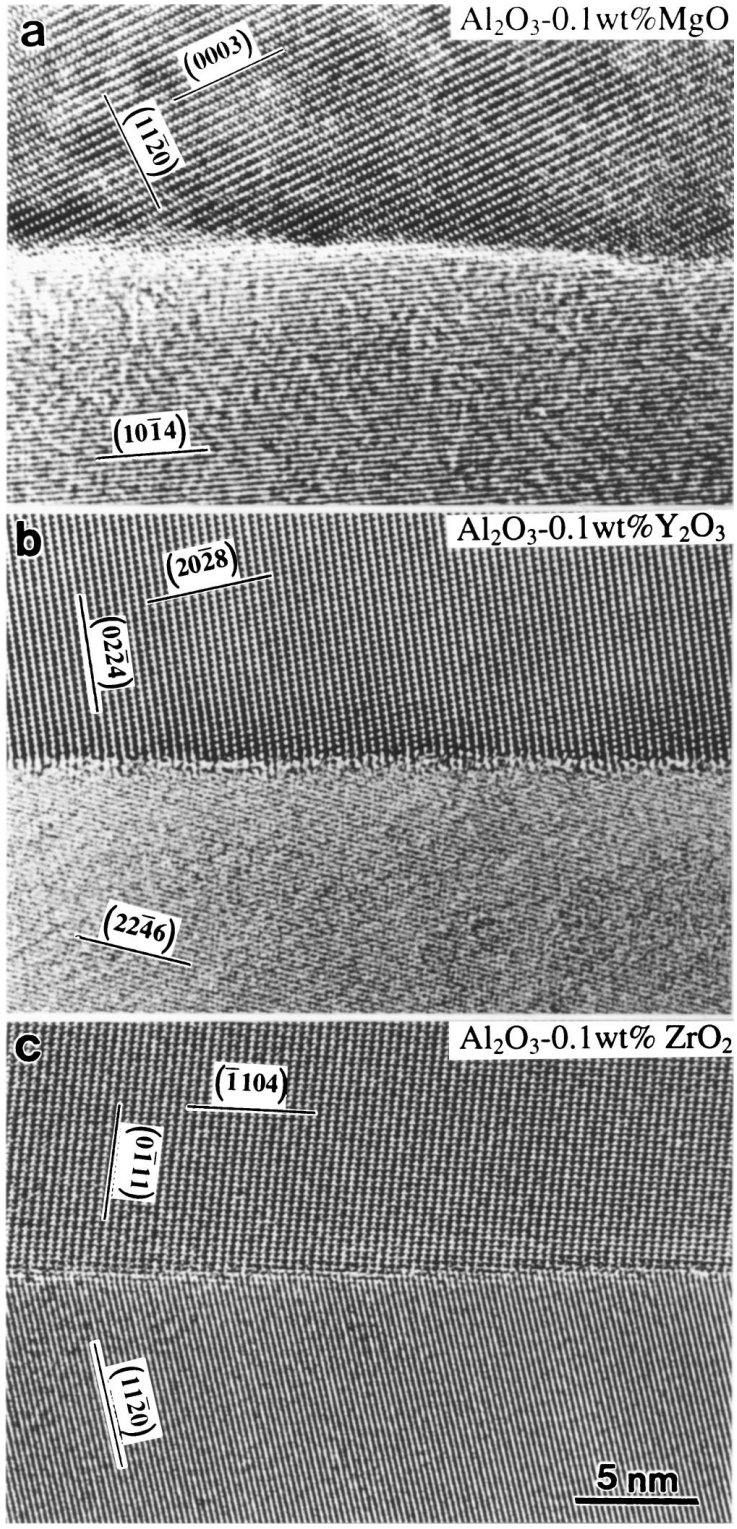

Figure 2 HREM image of a grain boundary in (a) MgO-doped Al_2O_3, (b) Y_2O_3-doped Al_2O_3 and (c) ZrO_2-doped Al_2O_3.

value of K_{Ic}. The K_{Ic} value is calculated by the following equation [12];

$$K_{Ic} = \left(\frac{PS}{BW^{3/2}}\right)\left\{\frac{3}{2}\left(\frac{a}{W}\right)^{1/2} Y\right\} \quad (1)$$

$$Y = \frac{\left[1.99 - \frac{a}{W}\left(1-\frac{a}{W}\right)\left\{2.15 - 3.93\frac{a}{W} + 2.7\left(\frac{a}{W}\right)^2\right\}\right]}{\left(1+2\frac{a}{W}\right)\left(1-\frac{a}{W}\right)^{3/2}} \quad (2)$$

where P is the applied force, S is the span length of three point bending, B and W are breadth and width of the specimen and a is the notch length. The fracture energy γ was calculated from the obtained K_{Ic} values by the following equation,

$$\gamma = \frac{K_{Ic}^2}{2E} \quad (3)$$

where E is the Young's modulus. In the bending tests, the tip radius of notch was about 50 μm in all samples. It has been reported that the measured K_{Ic} value in fine-grained Al_2O_3 is a little bit overestimated when the tip

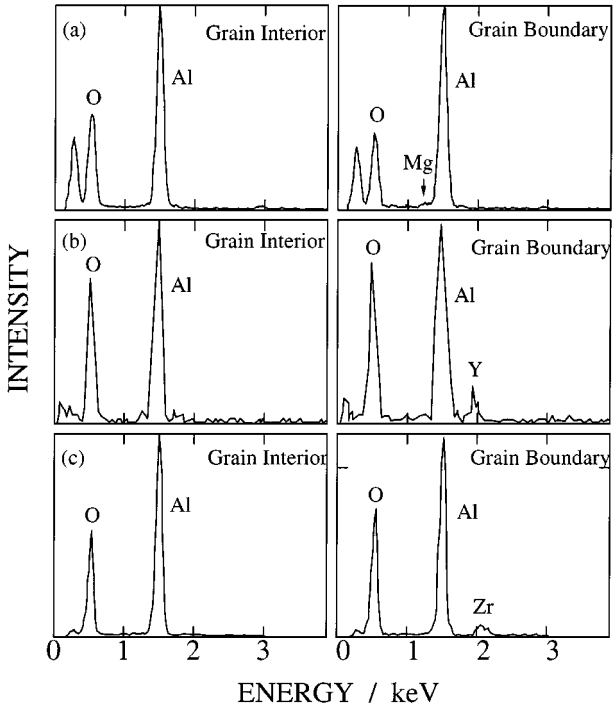

Figure 3 Typical EDS profiles obtained from a grain interior and a grain boundary in (a) MgO-doped Al_2O_3, (b) Y_2O_3-doped Al_2O_3 and (c) ZrO_2-doped Al_2O_3. The probe size for these analyses is about 1nm, and the spectra of grain interior were taken from the area 10 nm apart from the grain boundary.

radius is more than 10 μm [13]. However, the error has been estimated to be less than 10% when the tip radius is 50 μm in the report [13]. It has also been pointed out that fine-grained Al_2O_3 shows both transgranular and intergranular fracture at room temperature, but complete integranular fracture occurs above about 400 °C in three point bending [14]. The bending tests by SENB were then conducted at 400 °C to induce the perfect intergranular fracture. The temperature of 400 °C must be low enough to evaluate the fracture energy without the effect of diffusion in Al_2O_3.

Fig. 4 is the SEM micrographs of the fracture surfaces in (a) high-purity Al_2O_3, (b) MgO-doped Al_2O_3, (c) Y_2O_3-doped Al_2O_3 and (d) ZrO_2-doped Al_2O_3. The fracture surfaces consist of grain boundaries in all materials. Table I shows the comparison of the fracture energy estimated from K_{Ic} obtained in the four materials. In the estimation of fracture energy, the Young's modulus datum reported by Sakaguchi *et al.* was used [15]. The fracture energy obtained is in a range of 8 to 20 J/m^2. It has been reported that the fracture energy of Al_2O_3 is in a range between 10 and 40, and the value is about 10 for the grain size of about 1 μm [11, 16–19]. The values obtained in this study are within these reported values. As seen in Table I, the fracture energy of Al_2O_3 is dependent on the type of dopant.

TABLE I Comparison of fracture energy (γ) estimated from K_{Ic} obtained in high-purity Al_2O_3, MgO-doped Al_2O_3, Y_2O_3-doped Al_2O_3 and ZrO_2-doped Al_2O_3

	High-purity Al_2O_3	MgO-doped Al_2O_3	Y_2O_3-doped Al_2O_3	ZrO_2-doped Al_2O_3
γ (J/m^2)	12.7 ± 0.6	8.7 ± 0.9	19.9 ± 2.4	17.5 ± 3.0

As a factor to influence the fracture energy, the difference in grain size should be considered. The grain sizes are in the narrow range of 0.77 to 1.0 μm in the four materials. In addition, there is no correlation between fracture strength and grain size, i.e., the grain size is in the order of ZrO_2-doped Al_2O_3 > high-purity Al_2O_3 > MgO-doped Al_2O_3 > Y_2O_3-doped Al_2O_3, whereas the fracture energy is in the order of Y_2O_3-doped Al_2O_3 > ZrO_2-doped Al_2O_3 > high-purity Al_2O_3 > MgO-doped Al_2O_3. The grain size difference is not directly associated with the change in fracture energy in the present materials.

As shown in Fig. 4, the fracture occurs along grain boundaries in all materials. The obtained fracture energy must represent the grain boundary fracture energy. It has been proposed that the grain boundary fracture energy γ obtained by bending test is represented as the following equation [20, 21],

$$\gamma = \left(\gamma_s - \frac{1}{2}\gamma_{gb}\right) + \gamma_p + \gamma_d + \gamma_{etc} \qquad (4)$$

where γ_s is the surface energy, γ_{gb} is the grain boundary energy, γ_p is the energy for plastic deformation, γ_d is the energy for diversion of the crack and γ_{etc} is the other effects such as the energy for acoustic emission, the kinetic energy of the crack etc. Among the energy terms in Equation 4, $\gamma_s - 1/2\gamma_{gb}$ and γ_d are expected to change by the type of dopant. Since the doped cations segregate in grain boundaries, γ_{gb} must change by the type of dopant. Then, the term $\gamma_s - 1/2\gamma_{gb}$ is expected to change by the type of dopant. γ_d is also expected to change by the effect of segregated cations in grain boundaries because the diverted cracks consume the energy of $\gamma_s - 1/2\gamma_{gb}$ in each grain boundary. The origin of the change in grain boundary fracture energy seems to be associated with the segregated cations in grain boundaries. This result suggests that the segregated cations change the chemial bonding state in grain boundaries in Al_2O_3. The evaluation of the chemical bonding state will be discussed in the following section.

3.3. Chemical bonding state at grain boundaries

For evaluating the chemical bonding state, EELS is one of the most effective techniques especially in a narrow area such as grain boundaries. This is because the near edge structure of core-loss peaks in an EELS spectrum (electron energy loss near edge structure or ELNES) is sensitive to the structural and chemical environment of the atoms. The ELNES of the O-K edge is obtained from grain interiors and grain boundaries in the four materials. The EELS spectra are taken with the probe size of less than 1 nm. Fig. 5 shows the typical spectra of the O-K edge from a grain interior and a grain boundary for (a) high-purity Al_2O_3, (b) MgO-doped Al_2O_3, (c) Y_2O_3-doped Al_2O_3 and (d) ZrO_2-doped Al_2O_3. The peak energy is almost the same, but the fine structure of the peak around 540 eV differs slightly between the grain interior and the grain boundaries. The

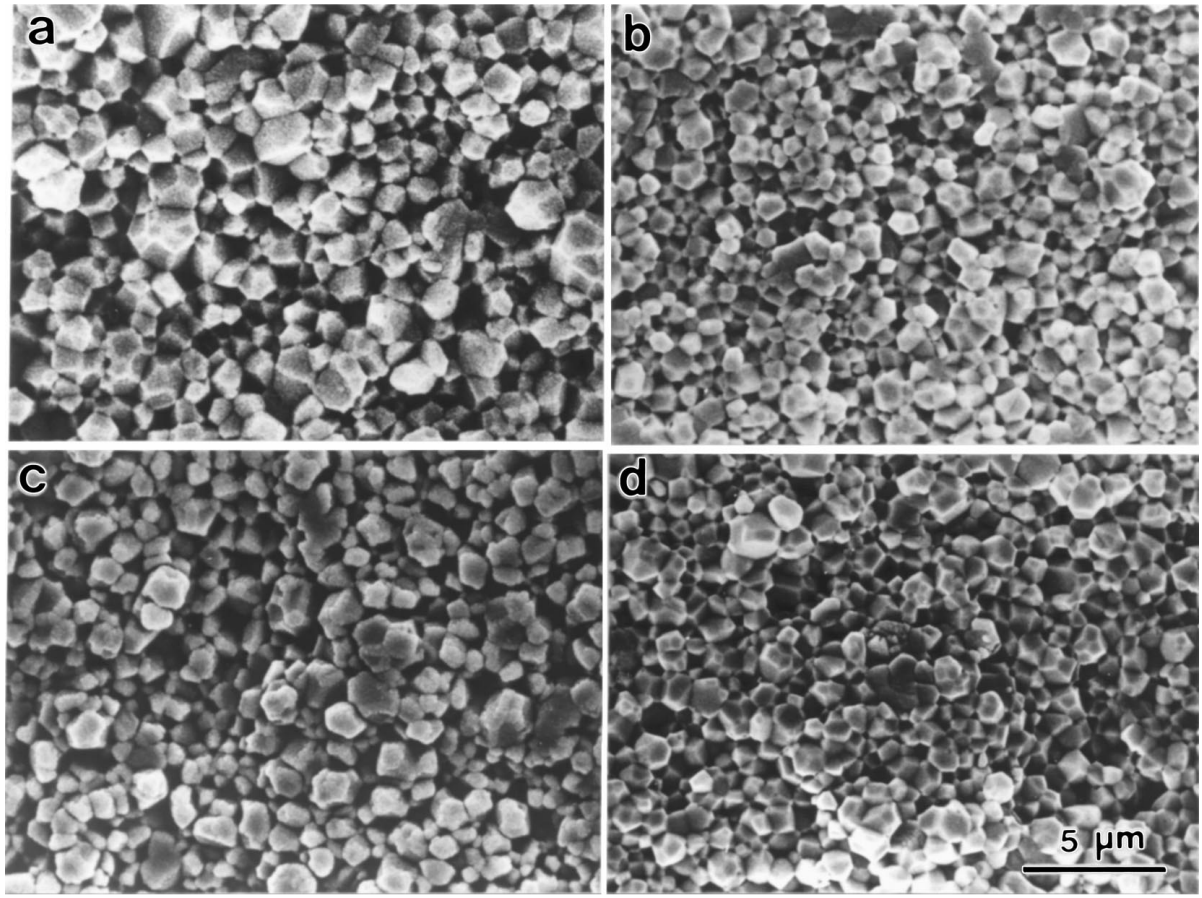

Figure 4 SEM micrographs of fracture surface in (a) high-purity Al_2O_3, (b) MgO-doped Al_2O_3, (c) Y_2O_3-doped Al_2O_3 and (d) ZrO_2-doped Al_2O_3, indicating that all specimens showed perfect intergranular fracture.

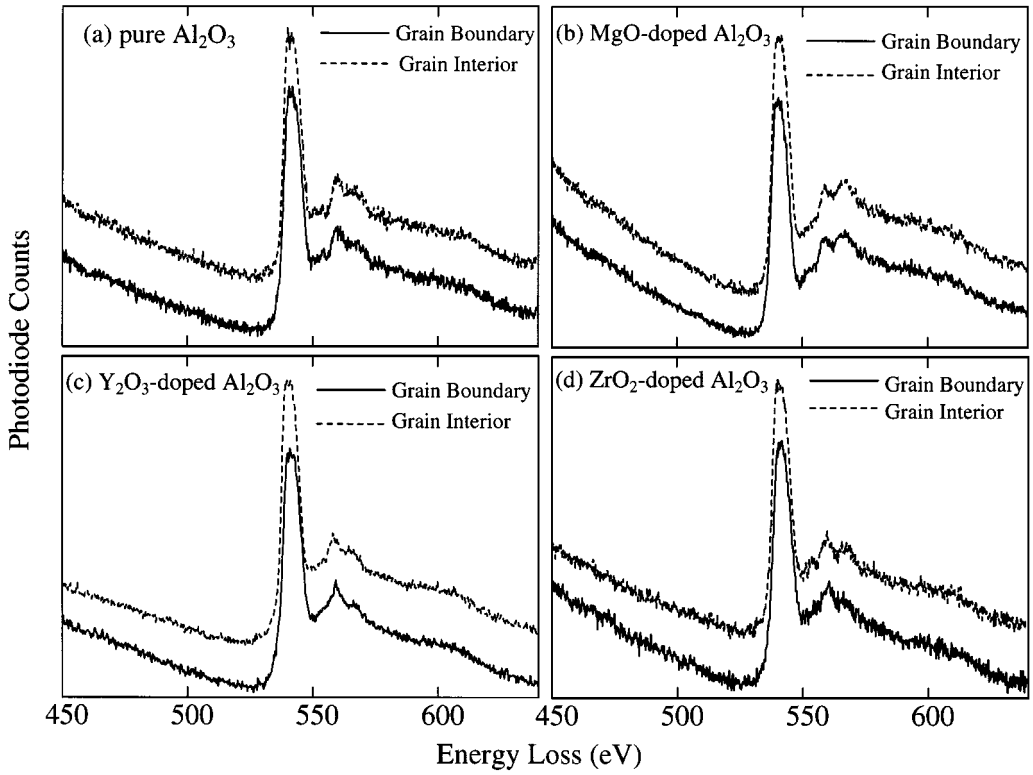

Figure 5 Typical EELS spectra of the O-K edge from a grain interior and a grain boundary for (a) high-purity Al_2O_3, (b) MgO-doped Al_2O_3, (c) Y_2O_3-doped Al_2O_3 and (d) ZrO_2-doped Al_2O_3.

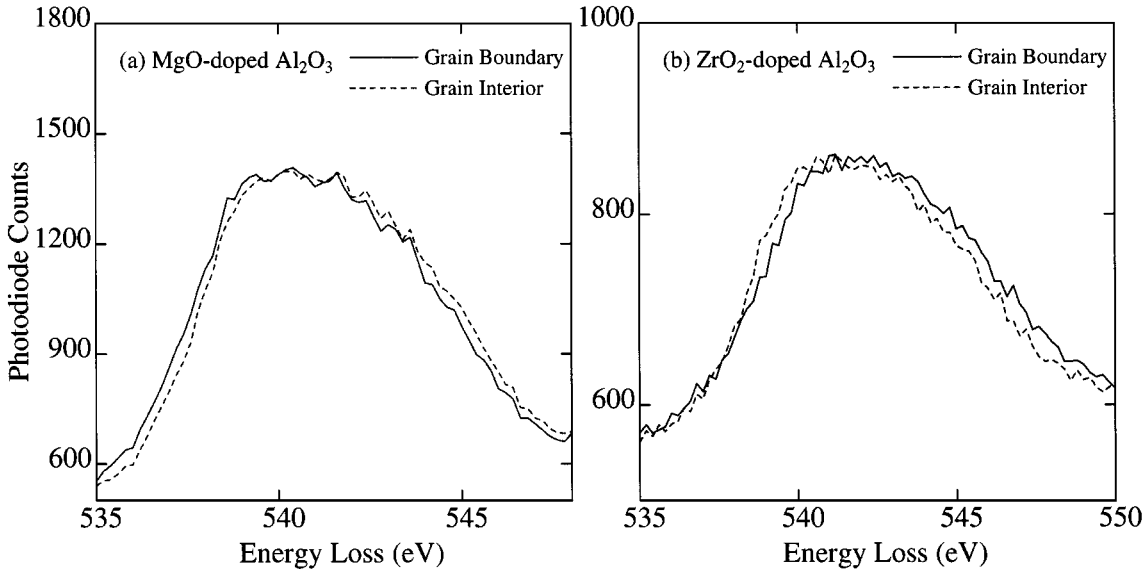

Figure 6 Comparison of EELS spectra of the O-K edge from a grain interior and a grain boundary in (a) MgO-doped Al_2O_3 and (b) ZrO_2-doped Al_2O_3.

difference in fine structure of the peaks is too weak to analyze quantitatively, but likely to refelct the atomic configuration at the grain boundries [22].

Fig. 6 is a comparison of the O-K edge peak in an enlarged scale between the grain interior and the grain boundary in (a) MgO-doped Al_2O_3 and (b) ZrO_2-doped Al_2O_3. The peak from the grain boundary slightly shifts to the lower energy side in comparison with that in the grain interior in MgO-doped Al_2O_3, while the peak from the grain boundary slightly shifts to the higher energy side in comparison with that in the grain interior in ZrO_2-doped Al_2O_3. The slight shift towards higher energy side is also observed in Y_2O_3-doped Al_2O_3. This tendency is always observed in other grain boundaries in all materials. Since such a chemical shift is not observed in high-purity Al_2O_3, the slight chemical shift in doped Al_2O_3 may correspond to the change in the chemical bonding state with the segregation of cations at grain boundaries. The electron-dipole selection rule allows the transition of oxygen from 1s orbital to 2p orbital in the case of O-K edge ELNES. As a result, the partial density of the state of O-2p corresponds to O-K edge ELNES [23]. Thus, the chemical shift suggests that the transition energy gap from O-1s to O-2p orbital decreases by the presence of Mg^{2+} ions, while it increases by the segregation of Y^{3+} or Zr^{4+} ions. It is difficult to explain macroscopic grain boundary energy from chemical bonding state, but, considering the fact that the grain boundary fracture energy is the smallest in MgO-doped Al_2O_3, the shift to lower energy side seems to correspond to the weakening of grain boundary bonding. On the other hand, the peaks of O-K edge ELNES obtained from grain boundaries in Y_2O_3 and ZrO_2-doped Al_2O_3 are slightly shifted to higher energy side in comparison with those obtained from grain interior as shown in Fig. 6. This agrees well with that both Y_2O_3 and ZrO_2-doped Al_2O_3 show high fracture energy if the shift to higher energy side would reflect the strengthening of the grain boundary bonding. Since the energy resolution of EELS is 0.7–0.8 eV in the present study, the amount of chemical shift can not be treated quantitatively, however, the tendency of chemical shift can be detected qualitatively as mentioned before. It is concluded that the change in chemical bonding state at grain boundary is likely to be an origin of the change in grain boundary fracture energy in oxide-doped Al_2O_3. However, in order to argue the chemical shift more quantitatively, the increase in energy resolution of EELS and theoretical calculation for the interpretation of the binding energy are necessary [24].

4. Conclusions

The grain boundaries in high-purity Al_2O_3, 0.1 wt % MgO-doped Al_2O_3, Y_2O_3-doped Al_2O_3 and ZrO_2-doped Al_2O_3 are characterized by estimating chemical composition, grain boundary fracture energy and chemical bonding state. The following results are obtained;

1. All materials examined in this study are identified to be single phase. The doped cations segregate along grain boundaries.
2. EELS spectra taken from grain boundaries in MgO-doped Al_2O_3 shifts to lower energy side in comparison with those from grain interior, while the spectra taken from grain boundaries in ZrO_2-doped Al_2O_3 shifts to higher energy side in comparison with those from grain interior. This result suggests that the chemical bonding state at grain boundaries changes by the type of dopant cations.
3. The grain boundary fracture energy of Al_2O_3 is affected by a small amount of dopant cation. The origin of the change in grain boundary fracture energy seems to be associated with the change in grain boundary bonding state by the segregation of dopant cation.

Acknowledgement

The authors would like to express their gratitude for the financial support of the Grant-in-Aid for Scientific Research on the Priority Area “Innovation in Superplasticity” (08242103) and for Fundamental Scientific

Research (09450256) from the Ministry of Education, Science and Culture, Japan. A part of this paper was also supported by Tokuyama science and technology research foundation. The useful discussions with Dr G. Pezzotti of Kyoto Institute of Technologies are acknowledged. We finally thank Topcon Co. Ltd. and JEOL Ltd. for the technical assistance of FE-TEM.

References

1. Y. YOSHIZAWA and T. SAKUMA, *Acta Metall. Mater.* **40** (1992) 2943.
2. F. WAKAI, T. IGA and T. NAGANO, *J. Ceram. Soc. Jpn.* **96** (1988) 1206.
3. H. YOSHIDA, Y. IKUHARA and T. SAKUMA, *Phil. Mag. Lett.* **76** (1997) 9.
4. Y. TAKIGAWA, Y. IKUHARA and T. SAKUMA, *Mater. Sci. Forum* **243–245** (1997) 425.
5. J. D. CAWLEY and J. W. HALLORAN, *J. Amer. Ceram. Soc.* **69** (1986) C195.
6. E. M. LEVIN and H. F. McMURDIE, "Phase Diagram for Ceramists," Vol. 3 (The Amer. Ceram. Soc. Inc., Westerville, Ohio, 1975) p. 135.
7. S. K. ROY and R. L. COBLE, *J. Amer. Ceram. Soc.* **51** (1968) 1.
8. J. J. GILMAN, *J. Appl. Phys.* **31** (1960) 2208.
9. D. HULL, P. BEARDMORE and A. P. VALINTINE, *Phil. Mag.* **12** (1965) 1021.
10. J. NAKAYAMA, *J. Amer. Ceram. Soc.* **48** (1965) 583.
11. H. G. TATTERSALL and G. TAPPIN, *J. Mater. Sci.* **1** (1966) 296.
12. J. E. SRAELY, *Int. J. Fract.* **12** (1976) 475.
13. T. NISHIDA, Y. HANAKI and G. PEZZOTTI, *J. Amer. Ceram. Soc.* **77** (1994) 606.
14. K. OKADA, PhD dissertation, The University of Tokyo, 1995.
15. S. SAKAGUCHI, M. MURAYAMA, Y. KODAMA and F. WAKAI, *J. Mater. Sci. Lett.* **10** (1991) 282.
16. R. D. DAVIDGE and G. TAPPIN, *J. Mater. Sci.* **3** (1968) 165.
17. J. A. COPPOLA and R. C. BRADT, *J. Amer. Ceram. Soc.* **56** (1973) 392.
18. T. NISHIDA and I. KAMEYAMA, *J. Ceram. Soc. Jpn.* **100** (1992) 276 (in Japanese).
19. T. KOYAMA, A. NISHIYAMA and K. NIIHARA, *J. Mater. Sci.* **29** (1994) 3949.
20. T. NISHIDA and T. NISHIKAWA, *Ceramics Japan* **20** (1985) 26 (in Japanese).
21. B. R. LAWN and T. R. WILSHAW, "Fracture of Brittle Solids" (Cambridge University Press, Cambridge, 1975).
22. M. M. DISCO, C. C. AHN and B. FULTZ, "Transmission Electron Energy Loss Spectrometry in Materials Science" (TMS, Warrendale, Pennsylvania, 1992).
23. I. TANAKA, J. KAWAI and H. ADACHI, *Solid State Commun.* **93** (1995) 533.
24. Y. IKUHARA, P. THAVORNITI, I. TANAKA and T. SAKUMA, *J. Electron. Micros.* **46** (1997) 467.

Received 27 October
and accepted 18 November 1998